

by

Kazuhiko Kawashima¹⁾, Shigeki Unjoh²⁾ and Hideyuki Shimizu³⁾**ABSTRACT**

This paper presents analytical and experimental studies on the dynamic characteristics of a variable damper developed at the Public Works Research Institute. Effectiveness of the variable damper for seismic response control of highway bridges is analytically investigated. A small-size model of the variable damper is developed and the dynamic characteristics through the dynamic loading tests is also presented.

KEY WORDS

Seismic Response Control, Highway Bridges, Variable Damper, Small-Size Model, Dynamic Loading Tests

1. INTRODUCTION

The variable damper^{1),2)} is a viscous damper in which the viscous damping force is variable depending on the response of highway bridges as shown in Fig.1. That is:

1) The damping coefficient of the variable damper is taken large during a small deck vibration so that the damper has the same function as a fixed bearing support against the braking load of vehicles. It is movable against actions with low-velocity such as an elongation of deck by temperature change.

2) When the amplitude of deck vibration becomes larger up to a certain level during an earthquake, the damping coefficient is decreased so that the energy dissipation be optimum and the inertia force of a superstructure to substructures be decreased appropriately.

3) Furthermore, when the vibration amplitude of the deck becomes excessive, the damping coefficient is gradually increased in order to suppress the excessive amplitude. Therefore, the damper has a function as a stopper with a shock absorber. This is to prevent the impact response by the sudden operation of the stopper⁴⁾.

Therefore, the variable damper has the advantages of an usual viscous damper stopper⁵⁾⁻⁷⁾, a passive energy dissipator and a stopper with a shock absorber function.

The concept of the variable damper, in which the damping characteristics can be variable dependent on the situation, has been effectively adopted in a field of mechanical engineering, in particular in a suspension system for an aircraft and an automobile. An active suspension to improve driving comfortability and stability of the automobile is one of the examples^{8),9)}. However, it is a new idea to apply the variable

damper for highway bridges based on the concept of distributing the inertia force of a superstructure to substructures.

Although various types of the variable damper can be made, the simplest one may be as shown in Fig.2. The basic component is an cylinder-type viscous damper. A by-pass pipe is installed between the cylinder-cells divided by the piston. The damping characteristics of the damper can be controlled by varying the amount of flow of viscous material which passes through the by-pass. Since various technology for controlling such material flow has been developed, the variable damper is most promising and near to the practical use. Furthermore, the external energy required for the operation is significantly smaller in the variable damper than in active control devices¹⁰⁾.

This paper presents analytical and experimental studies on the dynamic characteristics of a variable damper developed. The effectiveness of the variable damper for seismic response control of highway bridges is analytically investigated. A small-size model of the variable damper is developed and the dynamic characteristics through the dynamic loading tests is also presented.

2. SEISMIC RESPONSE ANALYSES OF HIGHWAY BRIDGES WITH VARIABLE DAMPERS**2.1 Seismic Response Analysis Method of Multi-Degree-of-Freedom System with Variable Dampers**

The equations of motion for a linear multi-degree-of-freedom system with the variable dampers may be written as

$$\underline{M} \ddot{\underline{x}} + (\underline{C} + \underline{C}_v) \dot{\underline{x}} + \underline{K} \underline{x} = - \underline{M} \ddot{\underline{x}}_0 \quad (1)$$

in which \underline{M} , \underline{C} and \underline{K} represent mass, damping and stiffness matrices of the system, respectively. \underline{x} and \underline{x}_0 denote displacement vector of the system and an earthquake ground motion, respectively. \underline{C}_v denotes a damping matrix of the variable dampers and is assumed as

- 1) Head of Earthquake Engineering Division, Earthquake Disaster Prevention Department, Public Works Research Institute, Ministry of Construction
- 2) Research Engineer, ditto
- 3) First Research Division, Fukushima Construction Office, Tohoku Regional Construction Bureau, Ministry of Construction (Formerly Assistant Research Engineer of the Earthquake Engineering Division, Public Works Research Institute)

$$\underline{C}_v = \sum_{k=1}^{n_v} \underline{c}_{ij} \dot{v} \quad (2)$$

where

$$\underline{c}_{ij} \dot{v} = \begin{bmatrix} V & -V \\ -V & V \end{bmatrix} \quad (3)$$

In which $\underline{c}_{ij} \dot{v}$ and n_v represent damping matrix of the variable damper, which is installed between the i -th node and the j -th node, and a number of the variable dampers installed, respectively. V is the damping coefficient of an each variable damper and is given as a function of relative displacement and relative velocity between the nodes where the variable dampers are installed.

Although there are various methods to prescribe the damping matrix \underline{C} , it is assumed here to be written as Eq.(4) assuming that the damping matrix \underline{C} can be diagonalized by the modal matrix.

$$\underline{C} = (\underline{\Phi})^{-1} \text{diag}[2h_k \omega_k] (\underline{\Phi}^T)^{-1} \quad (4)$$

In which, $\underline{\Phi}$ denotes a modal matrix of the system and $\text{diag}[2h_k \omega_k]$ denotes a diagonal matrix with elements of $2h_k \omega_k$ ($k=1,2,3,\dots$; mode number).

Since \underline{C}_v is time-varying, Eq.(1) has to be solved by a direct integration method. According to the above analytical method, a computer program "VDAM" which can analyze earthquake response of a multi-degree-of-freedom system with the variable dampers was developed.

2.2 Highway Bridge Analyzed and Analytical Conditions

In order to investigate the effectiveness of the variable damper, a simple span girder bridge, as shown in Fig.3, with a span length of 30m is analyzed. The response in longitudinal direction is considered. Although the variable damper has better applicability for multi-span continuous girder bridges, the simple span girder bridge is taken as an analytical model here for simplicity. The superstructure of the model is supported by elastic isolators in longitudinal direction and the variable dampers are assumed to be installed between the superstructure and the pier top.

The model can be assumed as a single-degree-of-freedom oscillator if it is assumed that the deformation of the superstructure is negligibly small and that the piers are idealized as a linear spring. Therefore, the damping coefficient of the variable damper, V , can be written as

$$V = \sqrt{m_d k_p} h_v \quad (5)$$

In which, m_d , k_p and h_v represent mass of the superstructure, a combined spring stiffness of elastic isolators and piers, and required

damping ratio for the variable damper, respectively. The weight of the superstructure and spring stiffness of the isolator are assumed as 241.5tf and 640tf/m, respectively. The flexural stiffness of piers is assumed so that the fundamental natural period of the model be 0.5sec when the both bearing supports are hinged. The stiffness of isolators result in the fundamental natural period of 1 sec for the model with elastic isolators.

Damping ratio of the variable damper h_v defined by Eq.(5) can be variable dependent on both relative velocity and relative displacement between the superstructure and the pier top. Only analytical cases in which the damping ratio is varied with the relative deck displacement are shown here for representing the effectiveness of the variable damper although the velocity-dependent variable damper was also studied.

Six cases in total are analysed as shown in Fig.4. In Case 1, the variable damper is not installed, i.e., no control. In Case 2, the damping coefficient of the damper h_1 is assumed independent on the relative deck displacement. The damping ratio h_1 is varied as a parameter to be investigated. Cases 3 and 4 are cases for investigating the effectiveness of the stopper with a shock absorber for preventing excessive deck displacement. The damping ratio increased from h_1 to h_3 dependent on relative deck displacement. In Case 3, a weak stopper, i.e., a stopper with a shock absorber is assumed and the damping ratio h_3 is assumed to be 3. In Case 4, the strong stopper is assumed and the damping ratio h_3 is assumed to be 500. The displacement at which the stopper initiates to work is assumed as 2/3 of the peak relative deck displacement d_u of Case 2. This displacement is defined hereafter as a design displacement of the variable damper. The design displacement of the variable damper d_d is 7.7cm as will be shown in Case 2. Case 5 is a case for investigating the effectiveness of the stopper for suppressing small deck displacement caused by vehicle loads. The damping ratio is increased from h_1 to h_2 in the range of the relative displacement from $-1/6d_u$ to $1/6d_u$. Case 6 is a combination of Cases 3, 4 and 5.

An acceleration ground motion shown in Fig.5 is used as an input acceleration. The acceleration, recorded on the ground around the Tsugaru Bridge during the Nihonkai-Chubu Earthquake of 1983, was modified so that the response spectrum matches with the target spectrum. The acceleration spectrum, which is specified in "Part V Seismic Design" of the "Design Specifications for Highway Bridges", for the check of bearing capacity of reinforced concrete piers on soft soil site (ground condition III), is assumed as the target spectra.

When the variable damper is not provided, the modal damping ratio of the model bridge is assumed to be 2% of critical in the above cases

2.3 Effectiveness of the Variable Dampers for Seismic Response Control of Highway Bridges

Fig.6 shows how the peak deck response and force developed at the pier vary in accordance with damping ratio h_1 for constant damping (Case 2). The peak deck displacement monotonously decreases with increasing the damping ratio h_1 and become almost stable for the damping ratio equal or greater than 2. The peak deck acceleration takes minimum at the damping ratio h_1 of about 0.5. This is because the function as a damper stopper becomes predominant rather than an energy dissipator. The shear force and bending moment at the pier bottom with increase of the damping ratio h_1 in a similar manner with the peak deck acceleration.

On the other hand, as the damping ratio increases the maximum damping force developed in the variable damper increases, while stroke of the piston decreases. Total energy dissipated during the excitation takes maximum value at the damping ratio of about 0.2.

Based on the analysis, the most appropriate damping ratio h_1 is considered as 0.5, which makes peak deck displacement and maximum bending moment at the pier bottom decrease to 31% and 37% of those with no control, respectively. The damping force and peak stroke of the piston required for this control are $34.7\text{tf} \times 2 = 69.4\text{tf}$ and 7.7cm, respectively.

Assuming h_1 as 0.5, the effectiveness of the stopper with a shock absorber was analysed. Fig.7 compares the deck displacement and acceleration as well as damping force of the variable damper for Cases 2 - 4. In Case 4, the pulse-type response developed by strong operation of the stoppers is seen in the damping force of the variable damper. Fig.8 compares the peak response and peak damping force for Case 2 - 4. Comparing Case 3 with Case 2, the peak deck response slightly decreases while maximum forces at the pier bottom increase only 7%. The maximum damping force of Case 3 developed in the variable damper becomes 1.73 times that of Case 2, and the peak stroke decreases by about 10%. The decrease of the stroke of the variable damper means that the function of the stopper operates effectively.

On the other hand, when the stopper operates strongly (Case 4) the responses become larger, and deck acceleration and forces at the pier bottom become about 2 times those in Case 3. Although the stroke of the variable damper decrease to the displacement at which the strong stopper operates, the peak damping force increase to about 4.3 times that in Case 3.

Fig.9 shows the effect of the stopper at the small deck displacement. The damping ratio of the damper, h_1 , is assumed to be 0.5 and h_2 is varied as a parameter. Although the peak deck displacement decrease monotonously as the damping ratio h_2 of the variable damper increases up to 8, it increases for the damping ratio h_2 greater than 8. This is because that the function

as a damper stopper becomes more predominant rather than an energy dissipator when the damping ratio h_2 becomes larger. The peak deck acceleration takes a minimum value when the damping ratio h_2 is about 1, and it increases monotonously for the damping ratio h_2 greater than 1. The forces at the pier bottom vary with h_2 in a similar manner with the deck acceleration.

On the other hand, as the damping ratio h_2 increases the damping force of the variable damper increases and the stroke and the total energy absorbed decrease. Therefore, damper at the small deck displacement which is for suppressing the deck motion caused by the vehicle loads has contrary effects to make seismic response smaller. Therefore, it is necessary to determine damping ratio h_2 in consideration with the function of bridges for normal loads.

Table 1 summarizes the peak responses in Case 1 to 6. If the variable damper with $h_1 = 0.5$ and $h_2 = h_3 = 3$ is provided, peak deck displacement and peak deck acceleration decrease 25% and 43% of those with no control, respectively. The maximum bending moment at the pier bottom decreases to 46% of that. The required damping force and peak stroke of the variable damper are $62.6\text{tf} \times 2 = 125\text{tf}$ and 5.78cm, respectively. The variable damper with this specification can be designed within the current scope of damper technology.

3. DEVELOPMENT OF A SMALL-SIZE MODEL OF THE VARIABLE DAMPER

3.1 Outline of A Small-Size Model of the Variable Damper

Fig.10 shows a design plan of the variable damper developed. The model is designed so that the damping force be variable in the range of 20kgf to 200kgf, maximum relative displacement of damper piston be within $\pm 2.5\text{cm}$. The control of the damping ratio is arbitrarily made by a personal computer dependent on relative displacement and velocity developed between deck and substructures.

The piston-cylinder has the total length of 394mm, the pressure area of the piston is 12.56cm^2 and the stroke of the piston is $\pm 2.5\text{cm}$. A steel pipe by-pass is installed between the cylinder-cells divided by the piston and the oil tank through two servo-valves. The servo-valve is called as a D.C. proportional magnetic valve, and the width of the valve is adjusted by the magnetic force of the D.C. proportional solenoid. The return spring is installed at the spool as shown in Fig.11. The differential transformer is installed at the servo-valve for the position detection of the spool so that the accurate control can be made. The input voltage from a servo amplifier to the servo valve is set in the range of 0 to 5V. The valve is closed at the input voltage of 0V and the valve is fully opened at

5V. The viscous material used for the variable damper is an usual oil for a dynamic loading actuator.

Fig.12 shows the flow of the viscous material in the variable damper. The damper piston can move in the left and right directions accompanying with the deck response. When the piston moves in the left side the viscous material flows from the left cell of the cylinder to the oil tank through the servo-valve 1, and from the tank to the right cell through the check valve 2 which can pass the oil only in one direction. At this time the servo-valve 2 is closed. When the piston moves in the opposite direction the oil passes through from cylinder to the tank through the servo-valve 2 and check valve 1. Therefore, the damping characteristics of the variable damper is controlled by the servo valve 1 when the piston moves in the left side, and by the servo-valve 2 when the piston moves in the right side.

3.2 Dynamic Loading Tests of the Small-Size Model of the Variable Damper

The variable damper can vary the damping characteristics depending on the displacement and/or velocity of the structures. Therefore, in order to provide the variable damper with the required damping characteristics it is necessary to know the basic dynamic characteristics of the variable damper. The damping characteristics of the variable damper is controlled by the amount of opening of the servo-valve and it is controlled by the input voltage to the servo-valve. Therefore, to know the characteristics of the variable damper developed, the relation between the input voltage to the servo-valve and damping characteristics of the variable damper is essential.

Fig.13 and Photo 1 show the set-up of the dynamic loading tests. The opening of the servo valve is kept to be constant under the condition that the input voltage is set to be a constant value, i.e., the damping ratio of the variable damper is set to be constant, the load is applied to the model by a dynamic actuator under the displacement control. The input voltage to the servo amplifier, reaction force and stroke of the piston are measured. The loading is harmonic and 10 cycle were repeated for each loading displacement.

Table 2 shows the experimental cases. Case 1 is to measure the friction force of the damper piston and static loading was made with loading frequency of 0.05Hz and loading displacement of 20mm. The input voltage of the variable damper is assumed to be 5V so as to open the valve fully. Case 2 is to obtain the input voltage to the servo-valve vs. damping force of the variable damper relation. Loading frequency, loading displacement and input voltage are varied.

3.3 Performance of the Small-Size Model of the Variable Damper

(1) Friction force of the damper-piston

Fig.14 shows a hysteresis loop of the load-displacement relation when the damper is loaded with the loading frequency of 0.05Hz and loading displacement of 20mm to obtain the friction force of the damper-piston. The load-displacement relation shows almost rectangular shape. This represents the typical type energy dissipation. The hysteresis is stable for a number of loading cycles. The average friction force was obtained as about 7kgf.

(2) Hysteresis Loops of the Load-displacement Relation

Fig.15 shows hysteresis loops of the load-displacement relation. In the loading displacement of 2mm, the time-lag was found in the peak damping force for the input voltage lower than 1.5V. This is developed due to compressibility and friction between the pipes and the viscous material. To compensate the effect it is required to make the pressure area greater for obtaining enough flow even if the displacement is small. In the loading displacement of 6mm and 10mm, the hysteresis loop seems as expected.

(3) The relation between the input voltage and damping force

Fig.16 shows the relation between the loading displacement and damping force dependent on the input voltage. The empirical equations obtained by a least square method are also shown in Fig.16. The relation between the damping force and loading velocity shows a function of the power of the loading velocity as an usual cylinder-type viscous damper. Therefore, the empirical equation is assumed as

$$F = F_0 + C(V) \cdot v^{n(V)} \quad (6)$$

where

F : damping force (kgf)

F_0 : friction force of the damper-piston (7kgf)

$C(V)$: damping coefficient (function of the input voltage V)

v : velocity of the damper-piston

$n(V)$: power coefficient of velocity term (function of the input voltage V)

In Eq.(6), damping coefficient $C(V)$, and power coefficient of velocity term $n(V)$, are unknown factors. They are computed by a least square method based on the tests results. The damping coefficient $C(V)$ thus obtained are almost constant in the range of the input voltage of 0 to 5V, and averaged value of $C(V)$ is 0.8. The relation between the input voltage and the power coefficient of the velocity term obtained is shown in Fig.17. The power coefficient increases with decrease of the input voltage. When the

input voltage is larger than 2.5V, the power coefficient becomes almost constant ($n(V) = 1.4$), and when the input voltage is lower than 2.5V the value takes larger. The relation obtained by a linear approximation is shown in Fig.17.

5. CONCLUDING REMARKS

The effectiveness of the variable damper developed for seismic response control of highway bridges was analytically investigated. The small-size model of the variable damper was developed and the performance was studied through the dynamic loading tests. According to the above investigations the following conclusions may be deduced:

1) In order to provide functions as damper stopper, energy dissipator and stopper with shock absorber for the variable damper, the damping ratio of $h_1 = 0.5$ and $h_2 = h_3 = 3$ is the most favorable.

2) By providing the variable damper with damping ratio shown in 1), the peak deck displacement and the peak deck acceleration of the model highway bridge were reduced to 25% and 43%, respectively. The peak bending moment decreased to 46%. The required peak damping force and peak stroke of the variable damper were $62.6\text{tf} \times 2 = 125\text{tf}$ and 5.78cm , respectively. The peak damping force is equivalent with 52% of the deck weight. These capability of the damper can be designed within the current scope of damper technology.

3) Based on the dynamic loading tests of the small-size model of the variable damper, the load-displacement relation was obtained as expected. A proto-type model of the variable damper is now under development for further improving the performance.

REFERENCES

- 1) Taguchi, J., Iwasaki, T., Adachi, Y., Sasaki, Y. and Kawashima, K. : U.S.-Japan Cooperative Research Program on Hybrid Control of Seismic Response of Bridge Structures, 22nd Joint Meeting, U.S.-Japan Panel on Wind and Seismic Effects, UJNR, Gaithersburg, Maryland, USA, May, 1990
- 2) Kawashima, K., Unjoh, S., Nagashima, H. and Shimizu, H. : Current Research Efforts in Japan for Passive and Active Control of Highway Bridges Against Earthquakes, 23rd Joint Meeting, U.S.-Japan Panel on Wind and Seismic Effects, UJNR, Tsukuba, May, 1991
- 3) Liu, S., C., Lagorio, H., J. and Chong, K., P. : Status of U.S. Research on Structural Control Systems, 23rd Joint Meeting, U.S.-Japan Panel on Wind and Seismic Effects, UJNR, Tsukuba, May, 1991
- 4) Kawashima, K., Hasegawa, K. and Nagashima, H. : Experiment and Analysis on Seismic Response of Menshin Bridges, Proc. 1st U.S.-Japan Workshop on Earthquake Protective Systems of Highway Bridges, National Center for Earthquake Engineering Research, Buffalo, N.Y., U.S.A., September 1991
- 5) Fukuoka, S. : Design of Multi-span Continuous Girder Bridge using Viscous Shear Stopper, Bridge, pp.22-29, February, 1980 (In Japanese)
- 6) Izeki, H. : Viscous Shear Stopper, Proposal to the Multi-Continuous Girder Bridge, Bridge, pp.30-33, February, 1980 (In Japanese)
- 7) Matsumura, S., Fukuoka, S., Mizumoto, Y. and Nakata, T. : Seismic Design of Multi-Span Continuous Girder Bridge using Damper Stopper, Bridge and Foundation, pp.31-37, May, 1982 (In Japanese)
- 8) Milliken, Jr., W., F. : Lotus Active Suspension System, Proceedings of 11th International Conference on Experimental Safety Vehicles, pp.467-475, Washington D.C., May, 1987
- 9) Sugawara, F. : Electronically Controlled Shock Absorber System Used as a Road Sensor which Utilizes Super Sonic Waves, Proceedings of Society of Automotive Engineers, pp.6.15-6.25, 1986
- 10) Kawashima, K., Unjoh, S. and Shimizu, H. : Optimum Seismic Response Control of Highway Bridges by Active Mass Damper, Civil Engineering Journal, Vol.33, No.9, pp.61-68, November, 1991 (In Japanese)
- 11) Kawashima, K., Unjoh, S. and Shimizu, H. : Earthquake Response Control of Highway Bridges by Variable Damper, Proceedings of Colloquium on Control of Structures, Japan Society of Civil Engineers, Part. B, pp.221-224, July, 1991 (In Japanese)
- 12) Feng, Q. and Shinozuka, M. : Use of A Variable Damper for Hybrid Control of Bridge Response Under Earthquake, U.S. National Workshop on Structural Control Research, University of Southern California, CA., U.S.A., October, 1990
- 13) Shinozuka, M., Feng, Q. and Kawamura, S. : New Perspectives for Sliding Base Isolation Systems, Proceedings of International Workshop on Recent Developments in Base-Isolation Techniques for Buildings, Tokyo, Japan, 27-30 April, 1992
- 14) Kawashima, K., Unjoh, S. and Shimizu, H. : Earthquake Response Control of Highway Bridges by Variable Damper, Transactions of the Japan National Symposium on Active Structural Response Control, Japan Science Council, pp.311-317, March, 1992 (In Japanese)
- 15) Kawashima, K., Unjoh, S. and Shimizu, H. : Experimental Study on Dynamic Characteristics of Variable Damper, Transactions of the Japan National Symposium on Active Structural Response Control, Japan Science Council, pp.311-317, March, 1992 (In Japanese)

Table 1 Peak Response of the Bridge and the Variable Damper

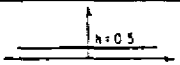
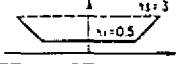
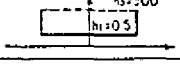
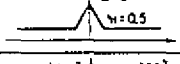
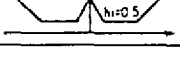
Analytical Cases	Deck			Pier		Variable Damper			
	Displacement (cm)	Velocity (cm/S)	Acceleration (cm/S ²)	Shear Force (tf)	Bending Moment (tf·m)	Damping Force (tf)	Relative Displacement (cm)	Relative Velocity (cm/S)	Total Energy (tf·m)
1 No Control	33.04	189.0	1300	166.9	3297	—	—	—	—
2 Constant Damping 	10.28	60.2	478	63.4	1223	34.7	7.67	44.9	93.9
3 Displacement Dependent Damping with Weak Stopper for Excessive Deck Response Displacement 	9.94	54.2	538	72.0	1395	60.2	6.90	68.1	94.4
4 Displacement Dependent Damping with Strong Stopper for Excessive Deck Response Displacement 	10.90	76.4	965	123.9	2382	151.3	5.54	112.3	94.9
5 Displacement Dependent Damping with Stopper for Small Deck Response Displacement 	8.50	51.3	567	80.1	1540	64.7	6.34	55.8	74.5
6 Displacement Dependent Damping (Combination of Case 3 and Case 4) 	8.38	47.5	555	81.2	1528	62.6	5.78	60.7	77.4

Table 2 Experiment for Small-Size model of Variable Damper

Case	Objective	Loading Frequency (Hz)	Loading Displacement (mm)	Input Voltage (V)
1	Measurement of Friction Force of Damper Piston	0.05	20	5
2	Relation between Damping Force and Input Voltage	1, 2, 3, 4	2, 6, 10, 15	0~5

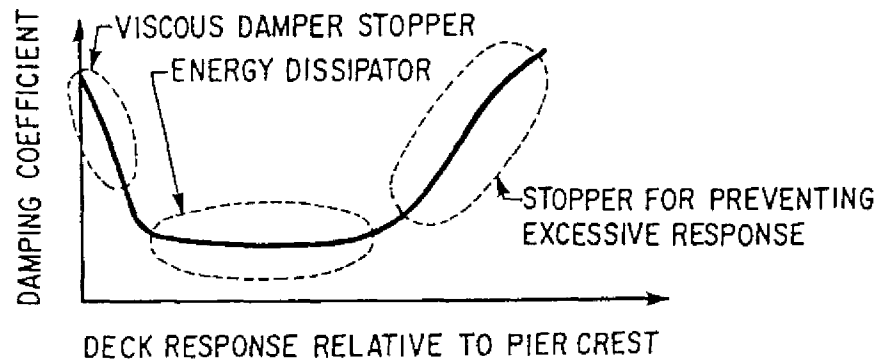


Fig.1 Basic Concept of Variable Dampers

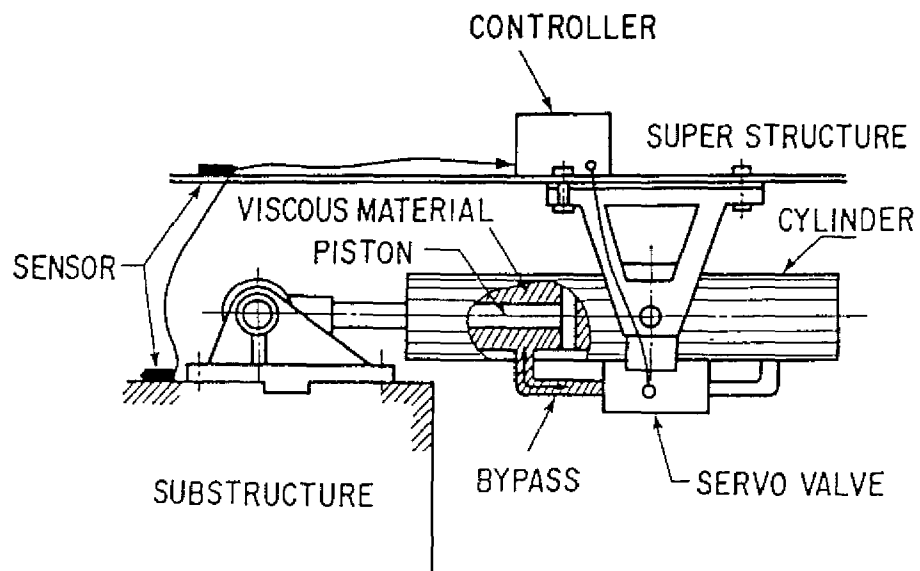


Fig.2 Variable Damper

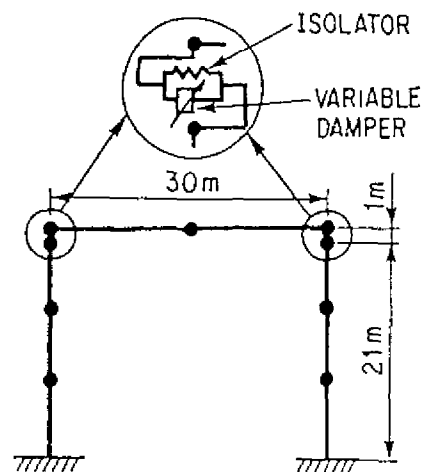
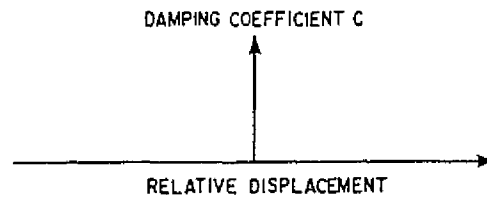
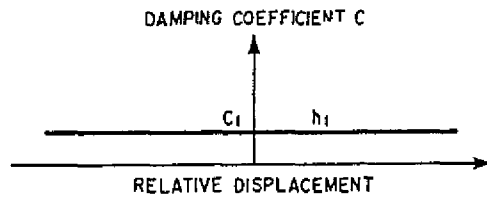


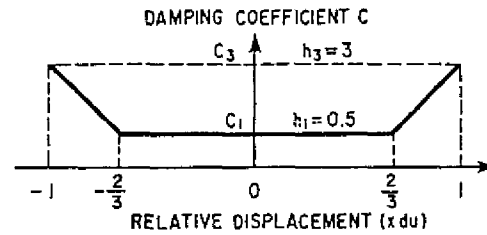
Fig.3 Highway Bridge Analyzed and Analytical Idealization



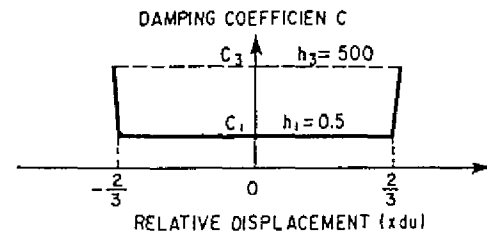
(a) Case 1 : No Control



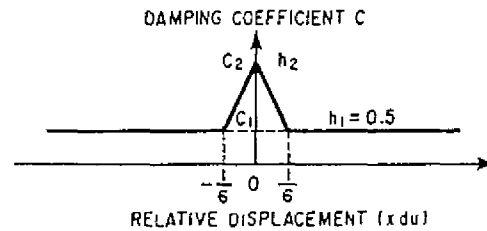
(b) Case 2 : Constant Damping



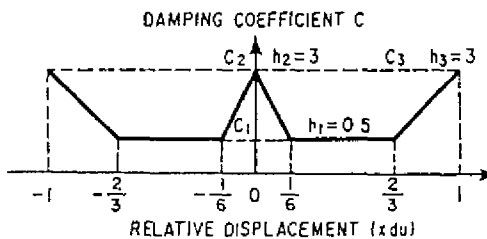
(c) Case 3 : Displacement Dependent Damping with Weak Stopper for Excessive Deck Response Displacement ($du=7.67\text{ cm}$)



(d) Case 4 : Displacement Dependent Damping with Strong Stopper for Excessive Deck Response Displacement ($du=7.67\text{ cm}$)



(e) Case 5 : Displacement Dependent Damping with Stopper for Small Deck Response Displacement ($du=7.67\text{ cm}$)



(f) Case 6 : Displacement Dependent Damping (Combination of Case 3 and Case 5) ($du=6.34\text{ cm}$)

Fig.4 Analytical Cases

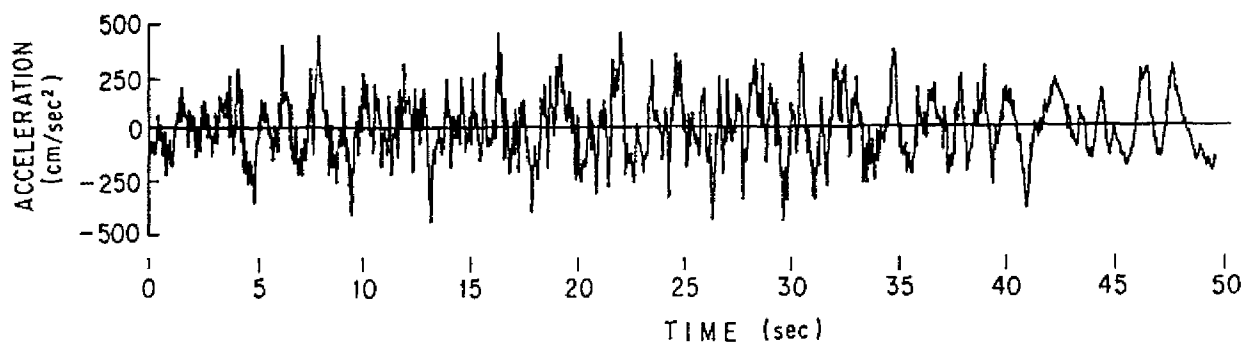


Fig.5 Input Acceleration

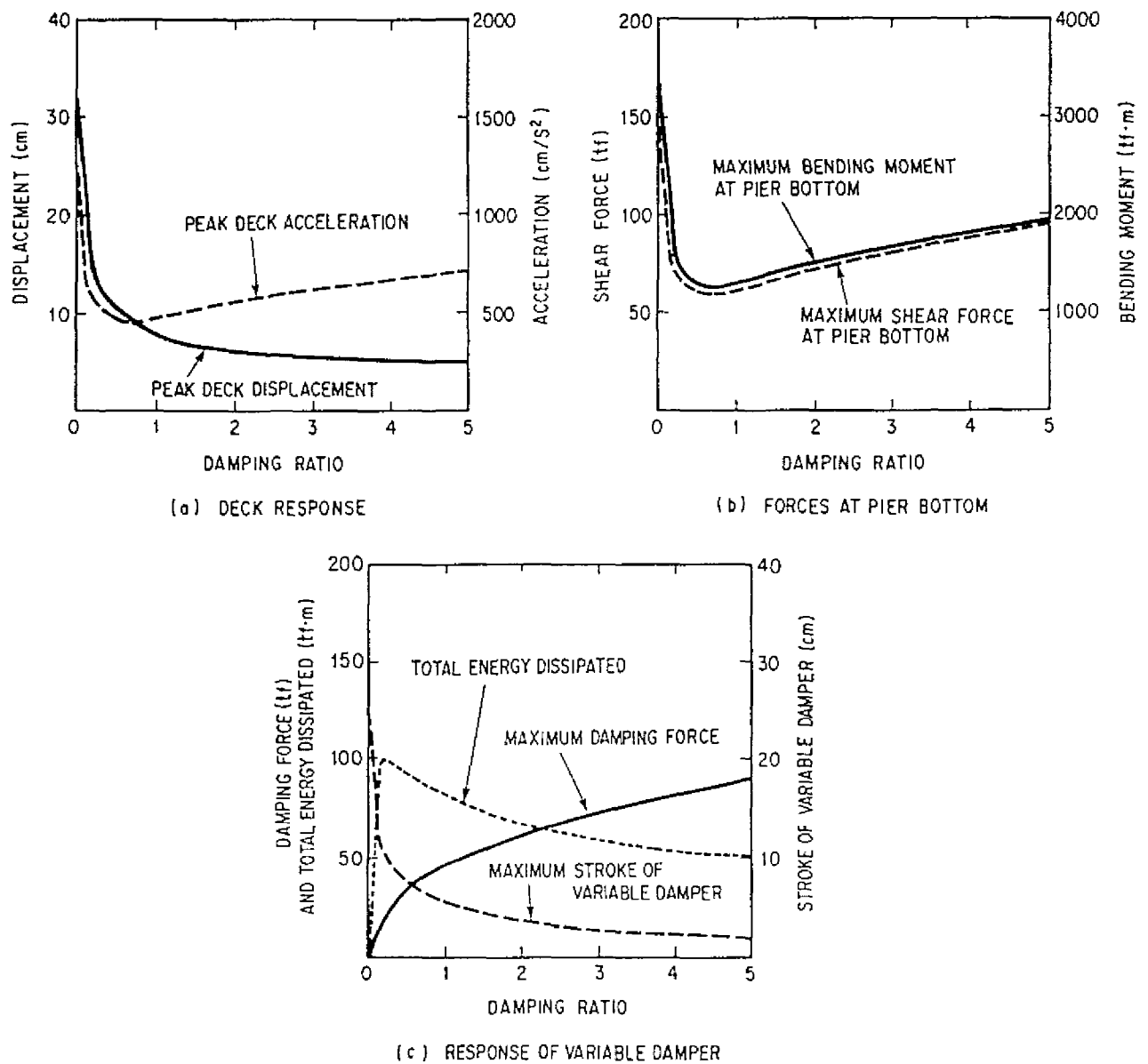


Fig.6 Peak Response of the Bridge and the Variable Damper (Case 2)

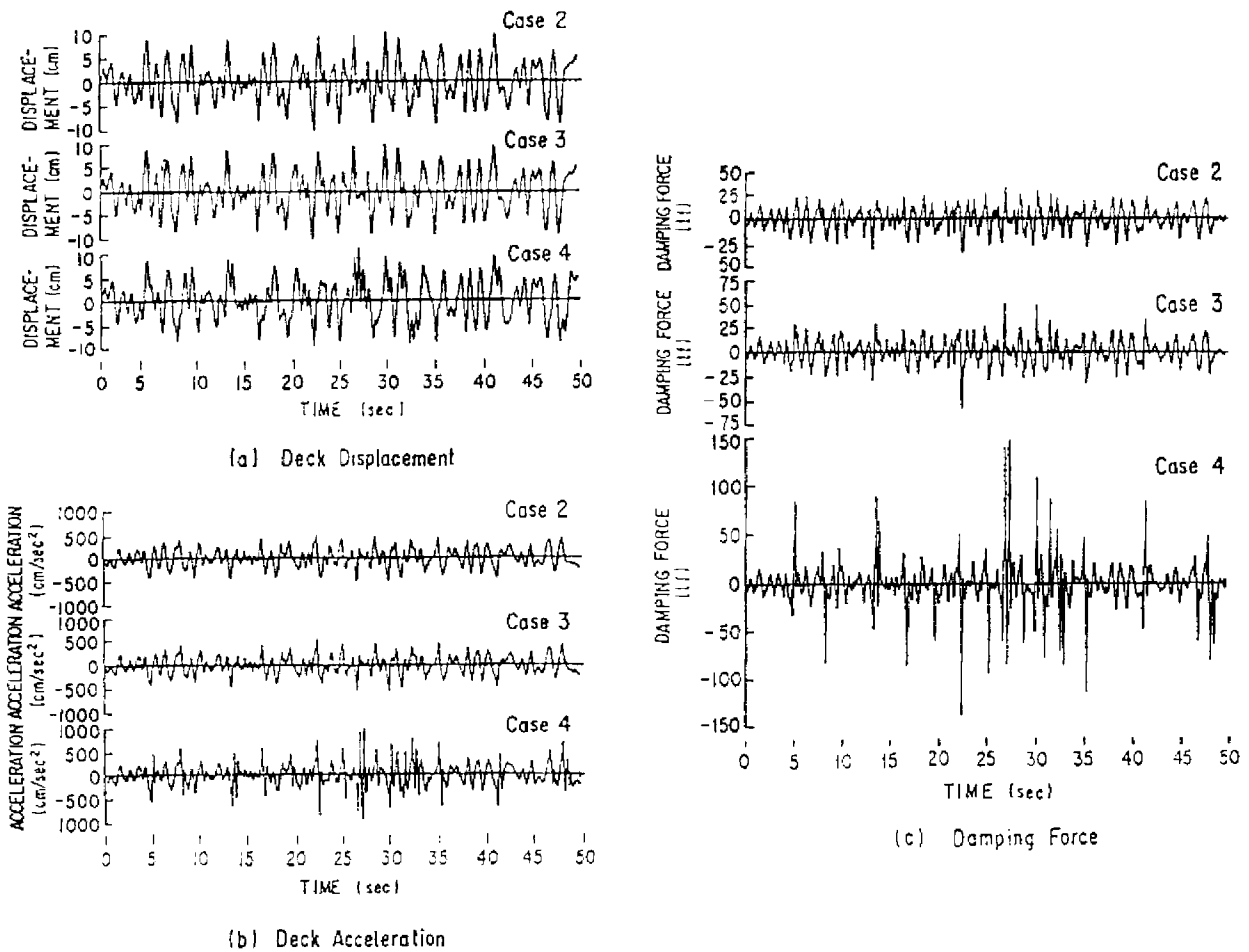


Fig.7 Computed Response of the Bridge and Variable Damper

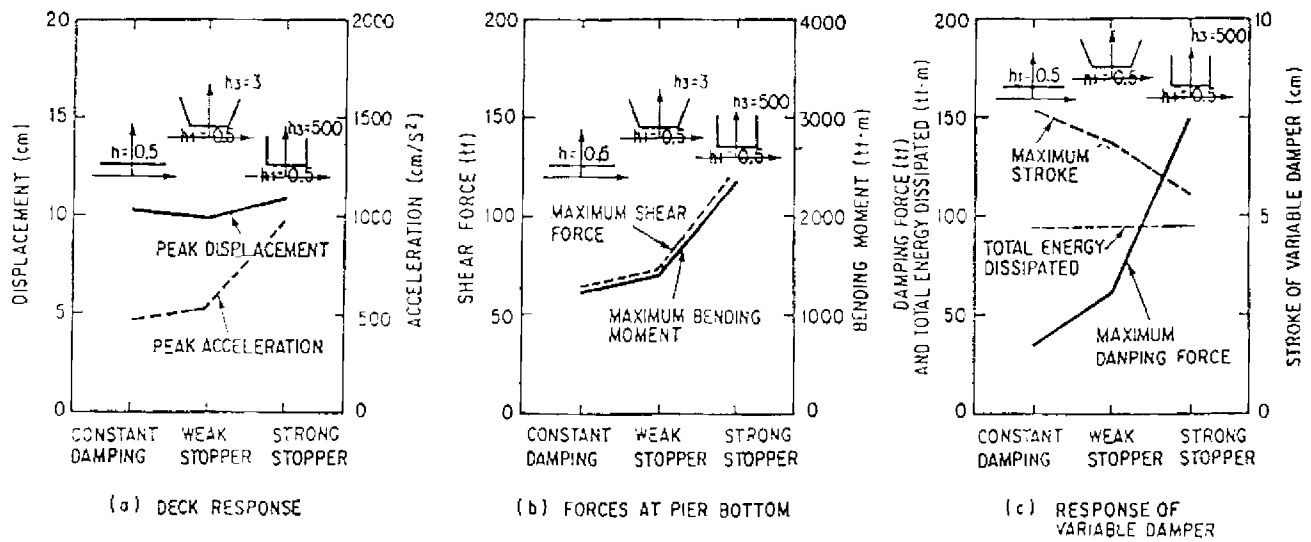
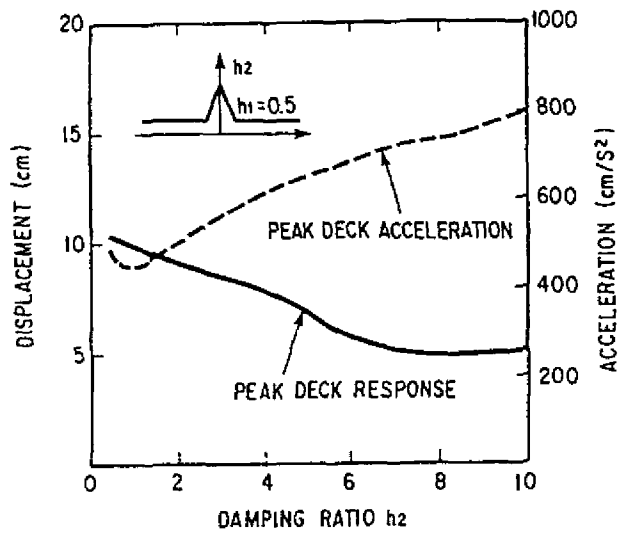
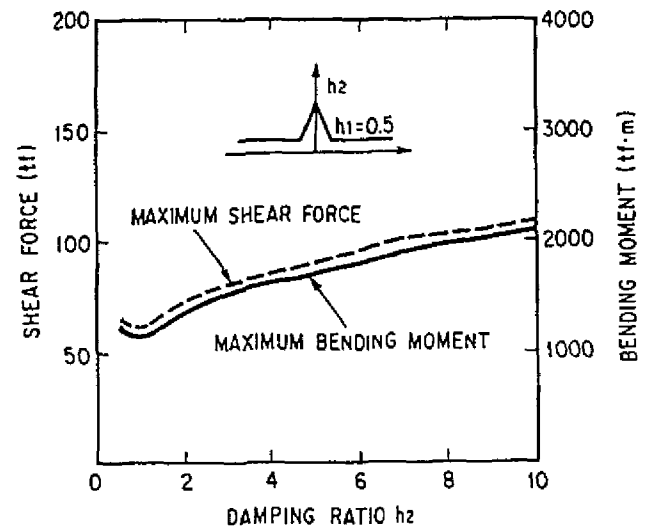


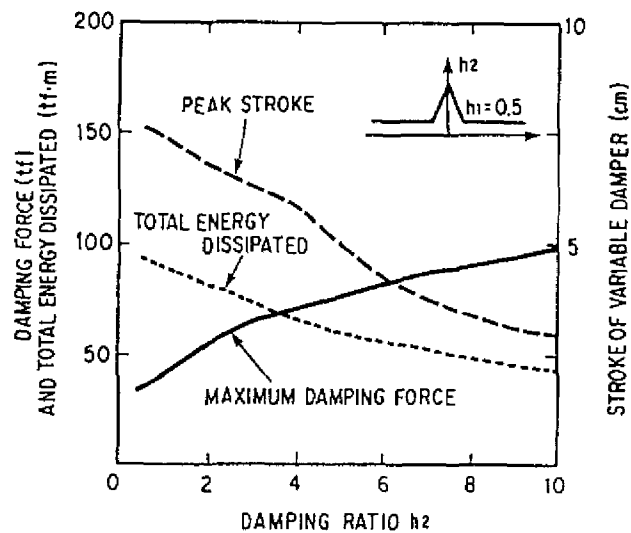
Fig.8 Effect of Weak Stopper (Case 3) and Strong Stopper (Case 4) for Excessive Deck Response Displacement



(a) DECK RESPONSE



(b) FORCES AT PIER BOTTOM



(c) RESPONSE OF VARIABLE DAMPER

Fig.9 Effect of Stopper for Small Deck Response Displacement (Case 5)

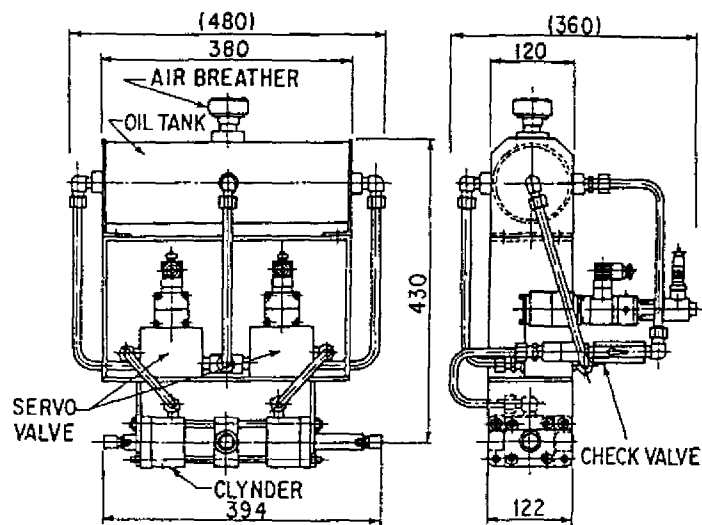


Fig.10 Small-Size Model of Variable Damper

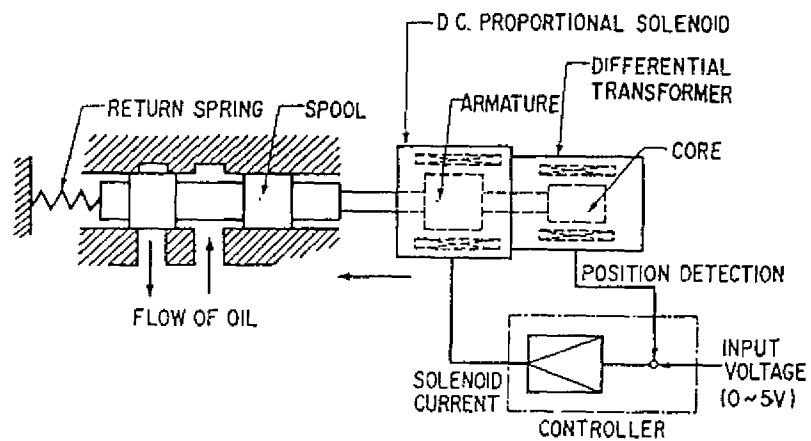


Fig.11 Structure of Servo Valve

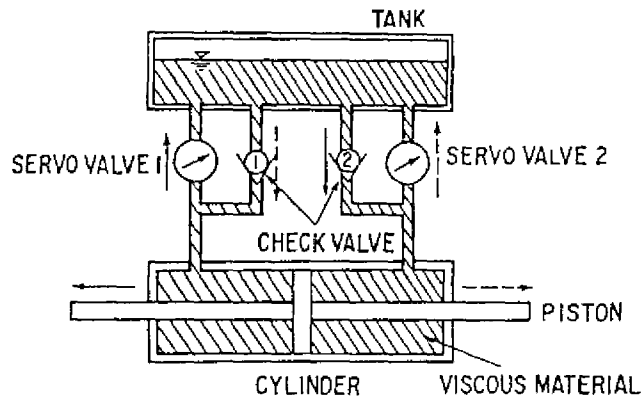


Fig.12 Flow of Viscous Material

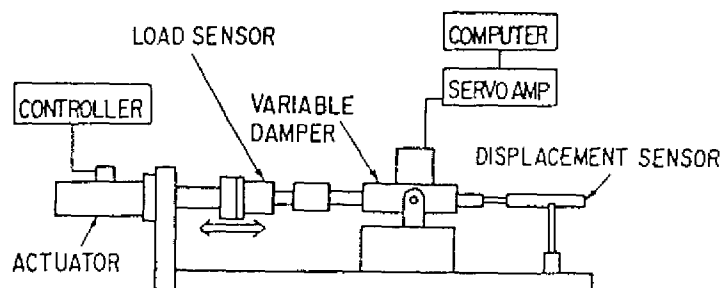
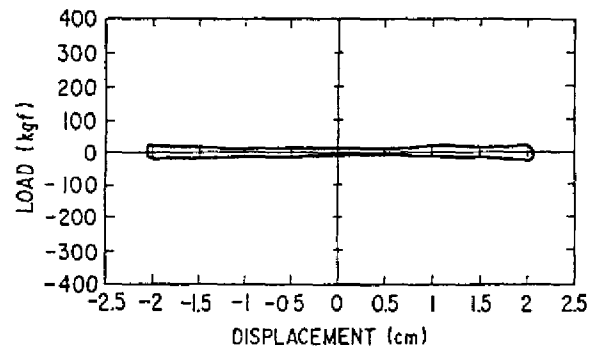
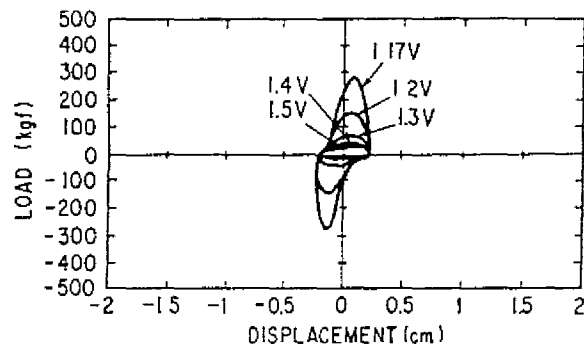


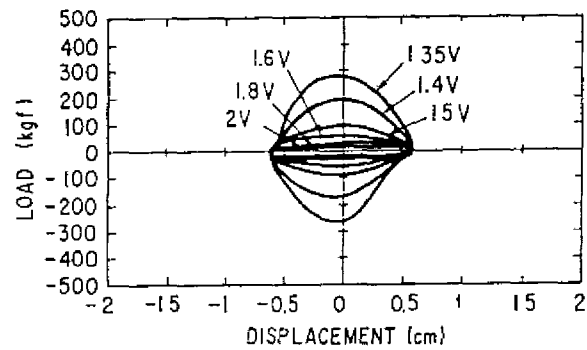
Fig.13 Set Up of Loading Test



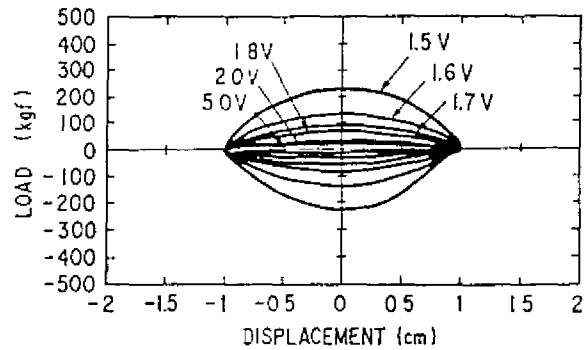
**Fig.14 Hysteresis Loops of Load-Displacement Relation
(Displacement=20mm, Frequency=0.05Hz)**



(a) Displacement 2mm



(b) Displacement 6mm



(c) Displacement 10 mm

**Fig.15 Hysteresis Loops of Load-Displacement Relation
(Frequency=1Hz)**

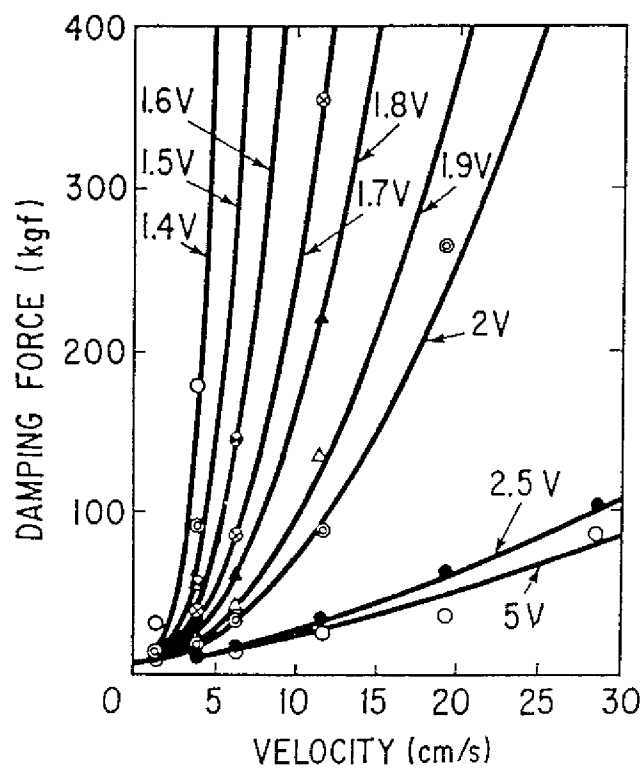


Fig.16 Damping Force vs. Peak Velocity Relation

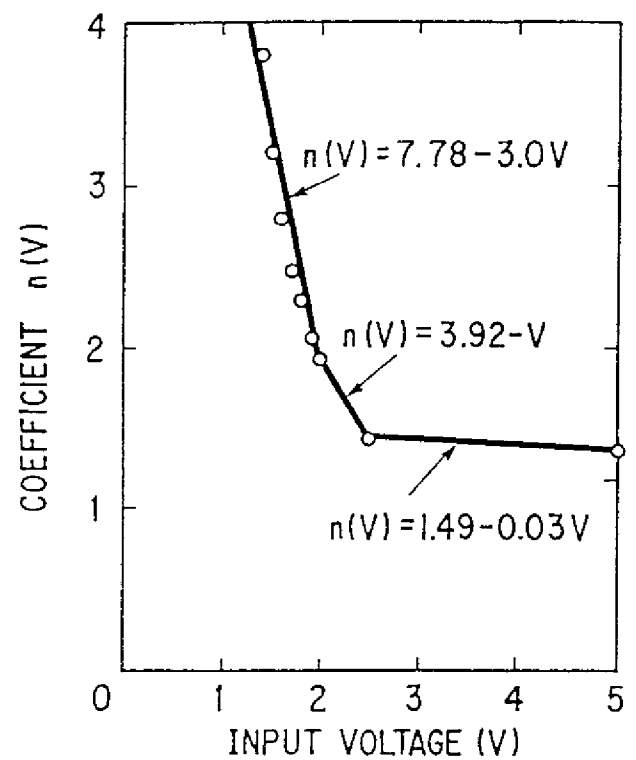


Fig.17 Power Coefficient $n(V)$ vs. Input Voltage Relation

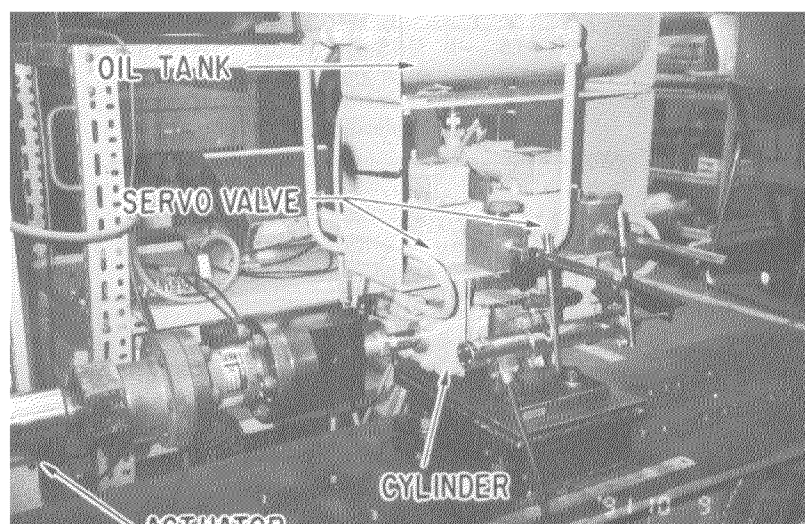


Photo 1 Experimental Set Up